NATURAL CONVECTION IN AN INCLINED POROUS TRIANGULAR ENCLOSURE WITH VARIOUS THERMAL BOUNDARY CONDITIONS

by

Sivanandam SIVASANKARAN[a*], Huey Tyng CHEONG[b,c], and Marimuthu BHUVANESWARI[d]

[a] Department of Mathematics, King Abdulaziz University, Jeddah, Saudi Arabia
[b] Institute of Mathematical Sciences, Faculty of Science, University of Malaya, Kuala Lumpur, Malaysia
[c] School of Mathematical Sciences, Sunway University, Sunway City, Malaysia
[d] Department of Mathematics, Kongunadu Polytechnic College, D. Gudalur, Dindigul, Tamil Nadu, India

Original scientific paper
https://doi.org/10.2298/TSCI160130159S

The aim of the study is to analyse the effect of two different thermal boundary conditions on natural convection in a porous triangular enclosure. Sinusoidal and linearly varying temperature profiles on the left wall are considered. The top wall of the enclosure is kept to be adiabatic. The Darcy model is adopted in this study and the governing equations are solved using the finite difference method for various values of inclination angle and Darcy-Rayleigh number. The results are presented in the form of streamlines, isotherms, and Nusselt numbers. The heat transfer rates are calculated and compared between two thermal boundary conditions. The heat transfer is more enhanced in the case of sinusoidal wall temperature than linearly varying wall temperature.

Key words: *natural convection, triangular enclosure, inclination, porous medium*

Introduction

Convective flow and heat transfer in porous enclosures are interested by many researchers due to its practical contributions in engineering, medical, geothermal, and other applications. These studies provide good understanding in circulation of cardiovascular system, design of solar collectors and geothermal systems. There are plenty of studies in enclosures with different geometries [1-3] under various conditions, like, radiation [4], external magnetic field [5], aspect ratio [6], variable fluid properties [7, 8], and rotating rod [9]. Aich *et al.* [1] examined natural convection in an isosceles prismatic enclosure and asymmetric flow structure is observed. Baytas and Pop [10] studied convection in an oblique cavity filled with porous medium. Later, Saeid and Pop [11] investigated transient free convection in a square porous enclosure. Sankar *et al.* [12] reported a study on different heating and cooling zones along the sidewalls in a square porous enclosure. Their work was then further extended by Bhuvaneswari *et al.* [13] to investigate the effect of aspect ratio on the convective flow in the partially heated and cooled porous enclosure.

Convection flow in triangular enclosures has been studied by several investigators [14-18]. Salmun [14] performed a numerical study in a triangular enclosure with various aspect ratios. Kent *et al.* [15] investigated convective flow in right triangular and quarter circular enclosures. The flow structures and heat transfer in a triangular enclosure with cold sidewalls

* Corresponding author, e-mail: sd.siva@yahoo.com

and heated bottom were analysed by Omri *et al.* [16]. Roy *et al.* [17] studied convection flow in an isosceles triangular enclosure with uniform and non-uniform heating at the bottom wall. Then, natural convective process inside the triangular enclosure filled with nanofluid was considered by Selimefendigil and Oztop [18]. The investigation on natural convection in triangular enclosures filled with porous medium has been performed by a few researchers [19-23]. Varol *et al.* [19] and Oztop *et al.* [20] studied the effect of aspect ratio in a porous triangular enclosure. Then, Varol *et al.* [21] studied the effect of inclination angle, φ, on convective flow in a porous triangular enclosure. They found that the local Nusselt number is maximum at $\varphi = 330°$ and minimum at $\varphi = 210°$. Basak *et al.* [22] investigated convective flow in a porous triangular enclosure with cold top wall and isothermally heated inclined sidewalls. Anandalakshmi *et al.* [23] performed a study on convective flow in a right-angled porous triangular enclosure. They observed that thermal mixing is reduced with linear heating of the sidewall.

The non-uniform thermal boundary conditions on natural convective flow were presented in several articles [24-30]. Natural convection in a porous cavity with sinusoidal bottom wall temperature was studied by Saeid [24]. It is found that the average heat transfer rate increases with increasing of the amplitude of the temperature profile. Basak *et al.* [25] investigated natural convection in a square porous enclosure with non-uniform heating at the bottom wall and constant cold sidewalls. Convective flow in an inclined porous triangular enclosure with heat generation and sinusoidal boundary conditions was investigated by Mansour *et al.* [26]. They concluded that increasing of enclosure inclination leads to the rise of horizontal velocity and Nusselt number. Sivasankaran and Bhuvaneswari [27] studied the effect of sinusoidal heating on the both sidewalls on convection in a porous enclosure. Later, Sivasankaran *et al.* [28] considered sinusoidal heating on the lid-driven enclosure. Also, partial heating on the square enclosure was considered by Nazara *et al.* [29] and Rahman *et al.* [30].

From the past researches, there is no study to compare the sinusoidal and linearly varying wall temperature on natural convection in a porous triangular enclosure. Hence the present study deals the natural convection in an inclined porous triangular enclosure subject to sinusoidal or linear temperature profile on one of the sidewall.

Mathematical formulation

Consider a 2-D triangular enclosure of height and width L filled with fluid saturated porous medium as shown in the fig. 1. The top wall of the enclosure is insulated. Temperature profile, $T(y)$, is applied on the left wall while the right wall is cooled with constant temperature, T_c. Two cases of temperature profile are considered in this study, which are sinusoidal wall temperature (SWT) and linear wall temperature (LWT). The inclination angle of the enclosure, φ, is the angle between the x-axis and the horizontal plane. The gravity acts in the vertical downward direction. The velocity components, u and v are taken in the x- and y-directions, respectively. The fluid in the enclosure is incompressible and Newtonian. The fluid properties are constant and the density variation is neglected except in the buoyancy term (by Boussinesq approximation). The porous medium is assumed to be homogeneous, isotropic and in thermal equilibrium with the fluid. Furthermore, we assume that the flow is steady and the viscous dissipation is negligible.

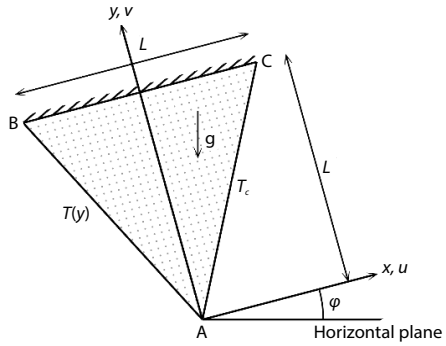

Figure 1. Schematic diagram

Hence, the Darcy model is adopted to explain the fluid-flow through the porous medium. By the law of conservation for mass, momentum, and energy, the governing equations are:

$$\frac{\partial u}{\partial x}+\frac{\partial v}{\partial y}=0 \tag{1}$$

$$u=-\frac{K}{\mu}\frac{\partial P}{\partial x}+\frac{K\beta \mathrm{g}}{\nu}\left(T-T_{\mathrm{c}}\right)\sin\varphi \tag{2}$$

$$v=-\frac{K}{\mu}\frac{\partial P}{\partial y}+\frac{K\beta \mathrm{g}}{\nu}\left(T-T_{\mathrm{c}}\right)\cos\varphi \tag{3}$$

$$u\frac{\partial T}{\partial x}+v\frac{\partial T}{\partial y}=\alpha\left(\frac{\partial^2 T}{\partial x^2}+\frac{\partial^2 T}{\partial y^2}\right) \tag{4}$$

The boundary conditions are:

$$\begin{aligned}
&\text{on AB}:\ u=v=0,\ T=\begin{cases}T_{\mathrm{c}}+\left(T_{\mathrm{ref}}-T_{\mathrm{c}}\right)\sin\left(\pi\dfrac{y}{L}\right) & \text{for SWT}\\ T_{\mathrm{c}}+\left(T_{\mathrm{ref}}-T_{\mathrm{c}}\right)\dfrac{y}{L} & \text{for LWT}\end{cases}\\
&\text{on CA}:\ u=v=0,\ T=T_{\mathrm{c}}\\
&\text{on BC}:\ u=v=0,\ \frac{\partial T}{\partial y}=0
\end{aligned} \tag{5}$$

The governing equations are then expressed in terms of stream functions which are defined as $u = \partial\psi/\partial y$ and $v = -\partial\psi/\partial x$. Then the following dimensionless variables are introduced:

$$X=\frac{x}{L},\ Y=\frac{y}{L},\ \Psi=\frac{\psi}{\alpha},\ \Theta=\frac{T-T_{\mathrm{c}}}{T_{\mathrm{ref}}-T_{\mathrm{c}}},\ \mathrm{Ra}_{\mathrm{D}}=\frac{K\beta \mathrm{g}\left(T_{\mathrm{ref}}-T_{\mathrm{c}}\right)L}{\alpha\nu} \tag{6}$$

where Ra_{D} is the modified Darcy-Rayleigh number based on the enclosure width, L.

Using eq. (6), the dimensionless governing equations and boundary conditions are:

$$\frac{\partial^2\Psi}{\partial X^2}+\frac{\partial^2\Psi}{\partial Y^2}=-\mathrm{Ra}_{\mathrm{D}}\left(\cos\varphi\frac{\partial\Theta}{\partial X}-\sin\varphi\frac{\partial\Theta}{\partial Y}\right) \tag{7}$$

$$\frac{\partial^2\Theta}{\partial X^2}+\frac{\partial^2\Theta}{\partial Y^2}=\frac{\partial\Psi}{\partial Y}\frac{\partial\Theta}{\partial X}-\frac{\partial\Psi}{\partial X}\frac{\partial\Theta}{\partial Y} \tag{8}$$

$$\begin{aligned}
&\text{on AB}:\ \Psi=0,\ \Theta=\begin{cases}\sin\pi Y & \text{for SWT}\\ Y & \text{for LWT}\end{cases}\\
&\text{on CA}:\ \Psi=0,\ \Theta=0\\
&\text{on BC}:\ \Psi=0,\ \frac{\partial\Theta}{\partial Y}
\end{aligned} \tag{9}$$

The heat transfer in the enclosure is measured by the Nusselt number. It shows the ratio of convection to conduction heat transfer. The local Nusselt number is calculated along the sidewall as $\mathrm{Nu}_{\mathrm{loc}} = -\partial\Theta/\partial N$ where N is the normal plane of the sidewall considered. The average Nusselt number on the sidewall is defined:

$$\overline{\mathrm{Nu}}_{\mathrm{h}} = \frac{1}{s}\int_0^S \mathrm{Nu}_{\mathrm{loc}}\,\mathrm{d}S$$

where s is the length of the sidewall and S is the tangential plane of the sidewall considered.

Solution procedure and code validation

The finite difference method is used to discretize eqs. (7) and (8) subject to boundary conditions (9). The discretized equations are solved using the Successive-Under Relaxation (SUR) method. In order to carry out computations using uniform grids in the X- and Y-directions, the height of a grid is the double of its width, so that the grid points are coincided with the inclined sidewalls of the triangular enclosure. A grid test was performed for $\mathrm{Ra_D} = 10^3$ without inclination angle in the range of 81 × 41 to 401 × 201 grids. It is found that the grid size of 321 × 161 is sufficient to perform the computation as good as the finer mesh sizes. The converged solution is obtained by the condition:

$$\sum_{i.j}\left|\xi_{i,j}^{n+1} - \xi_{i,j}^{n}\right| < 10^{-6}$$

where ξ is either Ψ or Θ and n denotes the iteration. The trapezoidal rule is used to calculate the average Nusselt number. The computer code is validated based on the previous literature using differentially heated square porous enclosure. It is seen from the tab. 1, the results predicted by current code agree well with the previous studies.

Table 1. Comparison of $\overline{\mathrm{Nu}}_{\mathrm{h}}$ or natural convection in a square porous cavity

References	$\mathrm{Ra_D} = 10^2$	$\mathrm{Ra_D} = 10^3$
Baytas and Pop [10]	3.160	14.060
Saeid and Pop [11]	3.002	13.726
Varol *et al.* [21]	–	13.564
Present study	3.101	13.280

Results and discussion

A numerical study is conducted to investigate the effect of thermal boundary conditions and inclination angle on convective flow and heat transfer in a porous-medium-filled triangular enclosure. The range of the Darcy-Rayleigh number, $\mathrm{Ra_D}$, considered is $10 \sim 10^3$ and inclination angle, $\varphi = 0° \sim 180°$. There are two temperature profiles under investigation, which are SWT (designated as Case 1) and LWT (Case 2).

Figure 2 shows the streamlines and isotherms for $\mathrm{Ra_D} = 10^2$ with comparison between SWT and LWT. Both temperature profiles affect the flow structure and temperature distribution in the triangular enclosure. The inclination of the enclosure also is a factor for the change of the flow structure and temperature distribution in the enclosure. For SWT, it can be seen that counter acting dual cells are forming in the enclosure. The clockwise cell dominates and occupies the majority of the cavity for $\varphi = 0°$ and 45°. At $\varphi = 90°$, two cells of opposite flow direction are observed with larger cell flowing in anticlockwise direction near the insulated wall. Anticlockwise flow is dominating the cavity for $\varphi = 135°$ and 180°. The small weak cell is formed at the corner of sidewall. The isotherm near the left wall clustered near the left wall and top position of the right wall, and forms the thermal boundary-layers along the left wall and top portion of the cold wall for $\varphi = 0°$ and 45°. For $\varphi \geq 90°$, the isotherms are more concentrated near the thermally active wall and bottom part of the cold wall. The thermal boundary-layers are formed near the left wall and bottom portion of the right wall. The formation of thermal boundary-layer shows the convection dominant heat transfer. For the case of LWT, single cell is formed for all inclination angle of the enclosure. The fluid is flowing in clockwise direction for φ = 0-90°. Anticlock-

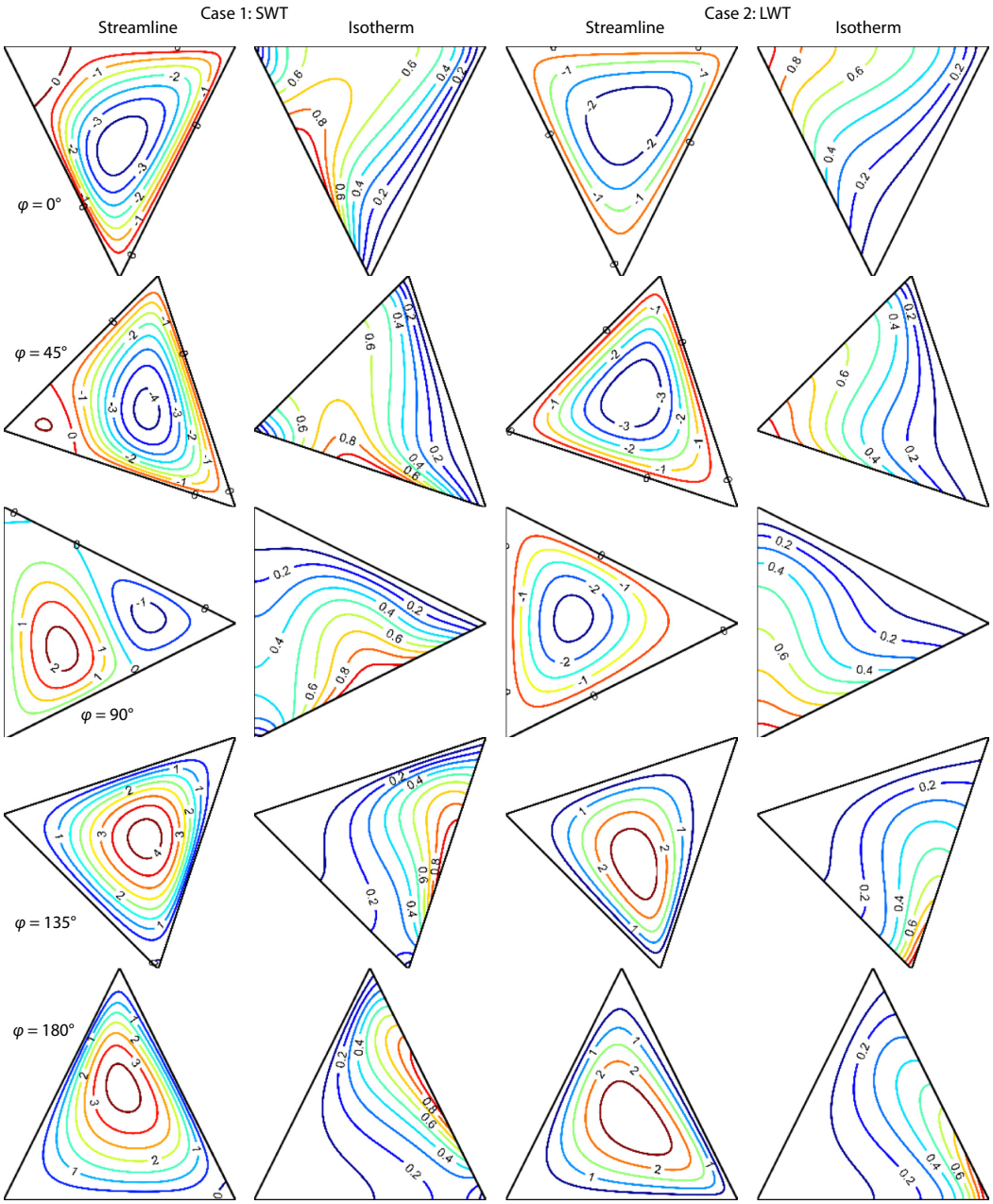

Figure 2. Streamlines and isotherms for various inclination angles with $Ra_D = 10^2$

wise flow is forming in the cavity with inclination $\varphi \geq 135°$. The isotherms are almost evenly distributed in the enclosure for φ = 0-90°. However, for $\varphi \geq 135°$, the isotherms are clustered at the top portion of the thermal active sidewall and thermal boundary-layers are formed at the top of the left wall.

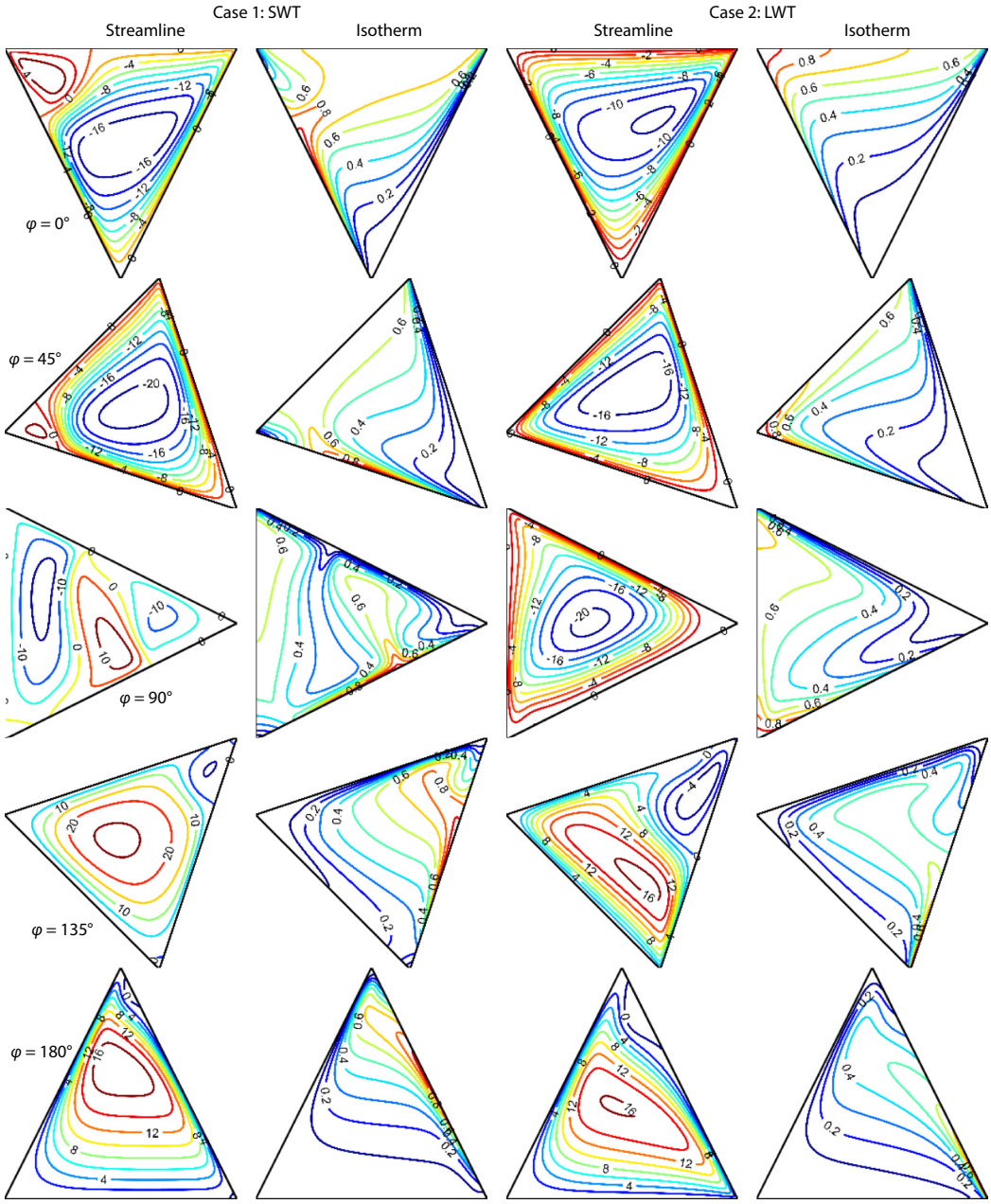

Figure 3. Streamlines and isotherms for various inclination angles with $Ra_D = 10^3$

The streamlines and isotherms for both cases with $Ra_D = 10^3$ are shown in the fig. 3. It is noticed that the Darcy-Rayleigh number affects the flow and temperature distribution in the cavity in comparison between figs. 2 and 3. Increasing the Darcy-Rayleigh number increases the ratio of buoyancy force to viscous force. Increasing effect of buoyancy force due to temperature difference in the enclosure drives the hot fluid to flow upwards at higher velocity.

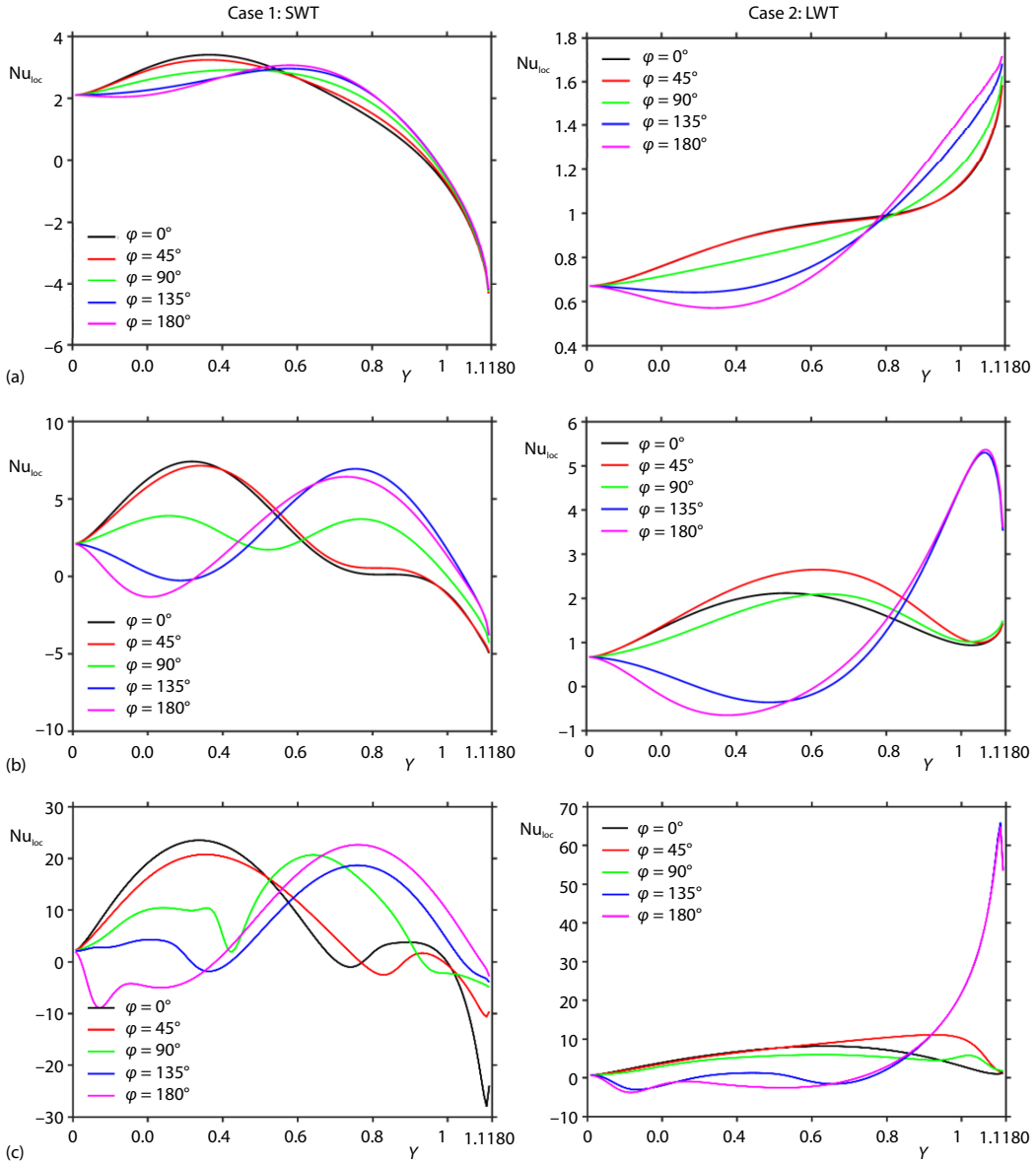

Figure 4. Local Nusselt number for (a) $Ra_D = 10$, (b) $Ra_D = 10^2$ and (c) $Ra_D = 10^3$

Decreasing fluid viscosity also causes the fluid to flow near to the walls of the enclosure. Therefore, the cell with high stream value is occupying a large area in the enclosure and it is closer to the boundary for $Ra_D = 10^3$ compared to $Ra_D = 10^2$. The isotherms show that convection is dominating the heat transfer in cavity with $Ra_D = 10^3$. The isotherms are closer to the active sidewall compared to $Ra_D = 10^2$, so the local heat transfer is higher for high Darcy-Rayleigh number. The flow phenomenon is similar to that of $Ra_D = 10^2$ for both cases, but there is another weak cell forming at the corner of the cavity for $\varphi = 135°$ and 180°. For $\varphi = 90°$ of LWT, it can be seen that two weak cells are formed near the thermal active sidewall.

Figure 4 shows the local heat transfer for SWT and LWT with $Ra_D = 10\text{-}10^3$. It can be seen from both cases that the variation of heat transfer along the thermal active sidewall depends on the temperature profile imposed and inclination of the enclosure. By considering SWT, the local heat transfer slightly increases near the bottom of the sidewall, and then it decreases along the wall for $Ra_D = 10$. However, the curves of the local heat transfer for $Ra_D = 10^2\text{-}10^3$ is of sine wave form. For $\varphi = 0°$ and 45°, the local heat transfer increases from the bottom wall to its global maximum around $Y = 0.3$, then it decreases along the wall. The trend of heat transfer for $\varphi = 135°$ and 180° is opposing of $\varphi = 0°$ and 45°, the local heat transfer increases from the bottom wall to its global maximum around $Y = 0.3$, then it decreases along the wall. The trend of heat transfer for $\varphi = 135°$ and 180° is opposing of $\varphi = 0°$ and 45° for $Y < 0.7$, where at the bottom of the sidewall, the local heat transfer decreases to its local minimum near $Y = 0.3$. Then, the local heat transfer increases and the global maximum is found around $Y = 0.7$. The local heat transfer is then decreasing along the wall. The local heat transfer for $\varphi = 90°$ is of wavy pattern, and increasing the Darcy-Rayleigh number increases the wavy sinusoidal heat transfer along the wall. Near $Y = 0.9$, the Nu_{loc} is negative for all Ra_D and φ. This indicates that the fluid in the enclosure is of higher temperature than the wall and heat is lost to the environment near the top of the thermally active wall. For LWT, heat is transferred into the enclosure with an increasing trend for $Ra_D = 10$. The Nu_{loc} for $\varphi = 0\text{-}90°$ increases gradually along the wall. It starts to decrease around $0.5 \leq Y \leq 0.8$ and slightly increases near the insulated wall. While $\varphi = 135°$ and 180°, the heat transfer decreases and at $Y = 0.7$, it increases rapidly to local maximum and decreases near the insulated wall. From fig. 4, it can be noticed that the maximum local heat transfer for SWT is higher than LWT for $Ra_D = 10$ and 10^2, but for $Ra_D = 10^3$, the maximum local heat transfer is higher for LWT. For $\varphi = 0\text{-}90°$, heat lost from the enclosure to environment for LWT is lower compared to SWT as the Nu_{loc} is positive.

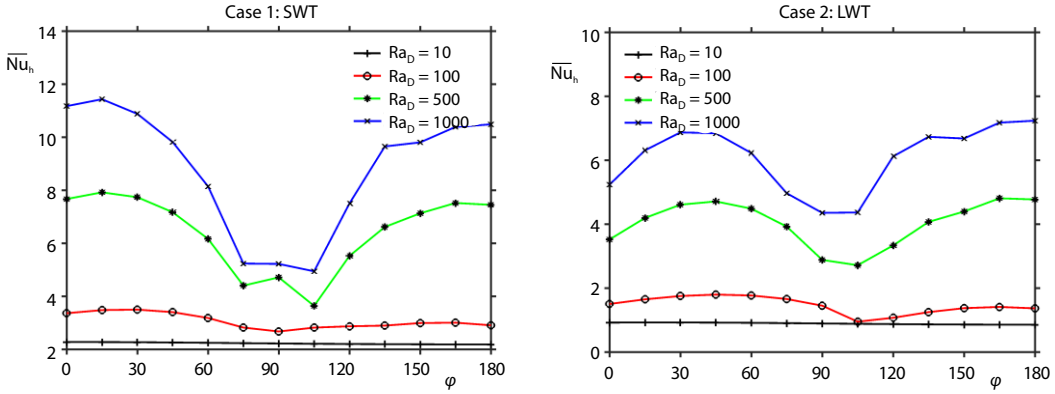

Figure 5. Average Nusselt number for different inclination angles and Ra_D

The average Nusselt numbers are shown in the fig. 5 with various Darcy-Rayleigh number and inclination angle. The average heat transfer increases with increasing of Darcy-Rayleigh number for all inclination angles. Figure 5 also shows that the heat transfer rates for SWT and LWT depend on the inclination of the enclosure. The variation of heat transfer with enclosure inclination for $Ra_D = 10$ is almost constant, and it shows the conduction-dominant regime across the fluid layer. For $Ra_D = 10^2\text{-}10^3$, both cases show similar pattern for heat transfer where it behaves non-linearly with the enclosure inclination. The plot of $\overline{Nu}_h$ is almost symmetrical at $\varphi = 90°$ for SWT. For $Ra_D = 10^2\text{-}10^3$, the lowest heat transfer for both

cases is found around $90° \le \varphi \le 105°$. However, the highest heat transfer for SWT is archived at $\varphi = 15°$ and for LWT is obtained at 45°. From fig. 5, it can be seen that the heat transfer is more enhanced for SWT compared to LWT.

Table 2. Comparison of $\overline{Nu}_h$ between SWT and LWT for various Ra_D and φ

φ	$Ra_D = 10$			$Ra_D = 10^2$			$Ra_D = 10^3$		
	SWT	LWT	Difference [%]	SWT	LWT	Difference [%]	SWT	LWT	Difference [%]
0°	2.28	0.93	59.4	3.37	1.51	55.2	11.18	5.24	53.1
15°	2.28	0.93	59.2	3.49	1.65	52.6	11.43	6.31	44.8
30°	2.27	0.93	59.1	3.50	1.76	49.8	10.88	6.87	36.9
45°	2.26	0.93	59.1	3.41	1.80	47.1	9.82	6.85	30.3
60°	2.25	0.92	59.2	3.19	1.77	44.3	8.15	6.23	23.6
75°	2.24	0.91	59.4	2.83	1.66	41.2	5.24	4.96	5.17
90°	2.23	0.90	59.6	2.68	1.45	45.7	5.22	4.36	16.6
105°	2.22	0.89	60.0	2.83	0.95	66.2	4.95	4.37	11.7
120°	2.21	0.88	60.2	2.87	1.08	62.5	7.51	6.13	18.4
135°	2.20	0.87	60.4	2.90	1.25	56.8	9.66	6.74	30.2
150°	2.20	0.87	60.6	3.00	1.38	54.0	9.81	6.68	31.9
165°	2.19	0.86	60.7	3.01	1.42	53.0	10.39	7.18	30.9
180°	2.19	0.86	60.8	2.91	1.37	52.9	10.49	7.24	31.0

Table 2 shows the comparison of $\overline{Nu}_h$ for SWT and LWT with various Darcy-Rayleigh number and enclosure inclination. The heat transfer of SWT is almost double of LWT for all inclination angle in $Ra_D = 10$. The enhancement of heat transfer depends on the cavity's inclination as shown by the differences of $Ra_D = 10^2$ and 10^3. The variation of difference is of wavy form with increasing inclination angle. Among all enclosure inclination considered, 0° has the highest difference and the least difference is found at 75°. For a fixed enclosure inclination, the difference of enhancement is decreasing by increasing Darcy-Rayleigh number. Therefore, SWT is more enhanced than LWT at low Darcy-Rayleigh number.

The correlation equations are derived based on data of $\overline{Nu}_h$ obtained from the simulation for different value of inclination angle and Darcy-Rayleigh number. For the case of SWT,

$$Ra_D = 10,\ \overline{Nu}_h = Ra_D^{-\frac{0.1}{\varphi+10}+0.45}\left(0.004\varphi^3 - 0.015\varphi^2 - 0.013\varphi + 0.83\right),\ 0 \le \varphi \le \pi$$

$$Ra_D = 10^2,\ \overline{Nu}_h = \begin{cases} Ra_D^{-\frac{0.1}{\varphi+10}+0.45}\left(0.077\varphi^4 - 0.21\varphi^3 - 0.074\varphi^2 - 0.020\varphi + 0.44\right), & 0 \le \varphi \le \pi/2 \\ Ra_D^{-\frac{0.1}{\varphi+10}+0.45}\left(-0.030\varphi^2 + 0.13\varphi + 0.23\right), & \pi/2 < \varphi \le \pi \end{cases}$$

$$500 \le Ra_D \le 10^3,\ \overline{Nu}_h = \begin{cases} Ra_D^{-\frac{0.1}{\varphi+10}+0.45}\left(0.36\varphi^4 - 0.97\varphi^3 + 0.60\varphi^2 - 0.095\varphi + 0.50\right), & 0 \le \varphi \le \pi/2 \\ Ra_D^{-\frac{0.1}{\varphi+10}+0.45}\left(-0.22\varphi^4 + 2.2\varphi^3 - 8.53\varphi^2 + 14.37\varphi - 8.61\right), & \pi/2 < \varphi \le \pi \end{cases}$$

The correlation equations for the case of LWT are:

$$\mathrm{Ra_D} = 10,\ \overline{\mathrm{Nu}}_\mathrm{h} = \mathrm{Ra_D}^{-\frac{0.1}{\varphi+10}+0.47}\left(0.002\varphi^3 - 0.011\varphi^2 + 0.006\varphi + 0.32\right),\ 0 \le \varphi \le \pi$$

$$\mathrm{Ra_D} = 10^2,\ \overline{\mathrm{Nu}}_\mathrm{h} = \begin{cases} \mathrm{Ra_D}^{-\frac{0.1}{\varphi+10}+0.47}\left(-0.023\varphi^4 - 0.065\varphi^3 - 0.095\varphi^2 + 0.085\varphi + 0.18\right), & 0 \le \varphi \le \pi/2 \\ \mathrm{Ra_D}^{-\frac{0.1}{\varphi+10}+0.47}\left(-0.023\varphi^2 + 0.14\varphi - 0.21\right), & 7\pi/12 < \varphi \le \pi \end{cases}$$

$$500 \le \mathrm{Ra_D} \le 10^3,$$

$$\overline{\mathrm{Nu}}_\mathrm{h} = \begin{cases} \mathrm{Ra_D}^{-\frac{0.1}{\varphi+10}+0.47}\left(0.13\varphi^4 - 0.40\varphi^3 + 0.24\varphi^2 - 0.073\varphi + 0.22\right), & 0 \le \varphi \le 7\pi/2 \\ \mathrm{Ra_D}^{-\frac{0.1}{\varphi+10}+0.47}\left(-0.070\varphi^4 + 0.42\varphi^3 - 0.38\right), & 7\pi/12 < \varphi \le \pi \end{cases}$$

Conclusion

The natural convection in an inclined triangular porous enclosure with sinusoidal and linearly heated wall has been studied. The governing equations and boundary conditions are solved directly by using the finite difference method. From the study, multiple flow patterns are observed for SWT case and single cell flow pattern is observed for LWT case. For small Rayleigh number, the heat transfer is dominated by conduction across the fluid layers, and then convection is dominated with increasing Darcy-Rayleigh number. The local Nusselt number is affected by the boundary conditions (SWT and LWT). The local Nusselt number is also affected by the enclosure inclination for $10^2 \le \mathrm{Ra_D} \le 10^3$. The average Nusselt number behaves non-linearly with inclination of the enclosure for all Darcy-Rayleigh number. The lowest heat transfer for SWT and LWT is found around $90° \le \varphi \le 105°$ while the highest heat transfer is found around $\varphi = 15°$ for SWT and $\varphi = 45°$ for LWT. It can be observed that the heat transfer is enhanced in the case of SWT than that of LWT. This study is useful for the understanding of convection process in the green house and solar heater.

Acknowledgment

The authors would like to acknowledge University of Malaya for the financial support through the Postgraduate Research Grant PG083-2014B.

Nomenclature

g – gravitational acceleration, [ms^{-2}]
H, *L* – enclosure height and length, [m]
K – permeability of the porous medium, [m^2]
$\mathrm{Nu_{loc}}$ – local Nusselt number (= $-\partial\Theta/\partial N$), [–]
$\overline{\mathrm{Nu}}_\mathrm{h}$ – average Nusselt number, [–]
P – pressure, [Pa]
$\mathrm{Ra_D}$ – Darcy-Rayleigh number [= $K\beta\, g(T_{ref} - T_c)L/\alpha\nu$], [–]
T – temperature, [K]
u, *v* – velocity components in *x*- and *y*-direction, [ms^{-1}]
x, *y* – Cartesian co-ordinates, [m]
X, *Y* – dimensionless Cartesian co-ordinates [= $(x, y)/L$], [–]

Greek symbols

α – thermal diffusivity, [m^{2}s^{-1}]
β – volumetric coefficient of thermal expansion, [K^{-1}]
μ – dynamic viscosity, [m^{2}s^{-1}]
ν – kinematic viscosity, [kgm^{-1}s^{-1}]
ψ – stream function, [m^{2}s^{-1}]
Ψ – dimensionless stream function (= ψ/α), [–]
Θ – dimensionless temperature [= $(T - T_c) / (T_{ref} - T_c)$], [–]

φ – inclination angle, [°]

Subscript

c – cold
ref – reference state

References

[1] Aich, W., *et al*., Numerical Analysis of Natural Convection in a Prismatic Enclosure, *Thermal Science, 15* (2011), 2, pp. 437-446
[2] Sourtiji, E., Hosseinizadeh, S. F., Heat Transfer Augmentation of Magnetohyrodynamics Natural Convection in L-Shape Cavities Utilizing Nanofluids, *Thermal Science, 16* (2012), 2, pp. 489-501
[3] Cho, C.-C., *et al*., Enchancement of Natural Convection Heat Transfer in a U-Shaped Cavity Filled with Al2O3-Water Nanofluid, *Thermal Science, 16* (2012), 5, pp. 1317-1323
[4] Kolsi, L., *et al*., Combined Radiation-Natural Convection in Three-Dimensional Verticals Cavities, *Thermal Science, 15* (2011), Suppl. 2, pp. S327-S339
[5] Sivasankaran, S., Bhuvaneswari, M., Effect of Thermally Active Zones and Direction of Magnetic Field on Hydromagnetic Convection in an Enclosure, *Thermal Science, 15* (2011), Suppl. 2, pp. S367-S382
[6] Chamkha, A. J., *et al*., Mixed Convection in a Partially Layered Porous Cavity with an Inner Rotating Cylinder, *Numer. Heat Transf. A*, *69* (2016), 6, pp. 659-675
[7] Cianfrini, M., *et al*., Natural Convection in Square Enclosures Differentially Heated at Sides Using Alumina-Water Nanofluids with Temperature-Dependent Physical Properties, *Thermal Science, 19* (2015), 2, pp. 591-608
[8] Salari, M., *et al*., Effects of Circular Corners and Aspect-Ratio on Entropy Generation Due to Natural Convection of Nanofluid Flows in Rectangular Cavities, *Thermal Science*, *19* (2015), 5, pp. 1621-1632
[9] Chang, B.-H., Numerical Study of Flow and Heat Transfer in Differentially Heated Enclosures, *Thermal Science, 18* (2014), 2, pp. 451-463
[10] Baytas, A. C., Pop, I., Free Convection in Oblique Enclosures Filled with a Porous Medium, *Int. J. Heat Mass Transf., 42* (1999), 6, pp. 1047-1057
[11] Saeid, N. H., Pop, I., Transient Free Convection in a Square Cavity Filled with a Porous Medium, *Int. J. Heat Mass Transf., 47* (2004), 8-9, pp. 1917-1924
[12] Sankar, M., *et al*., Buoyancy Induced Convection in a Porous Cavity with Partially Thermally Active Sidewalls, *Int. J. Heat Mass Transf., 54* (2011), 25-26, pp. 5173-5282
[13] Bhuvaneswari, M., *et al*., Effect of Aspect Ratio on Natural Convection in a Porous Enclosure with Partially Active Thermal Walls, *Comput. Math. Appl., 62* (2011), 10, pp. 3844-3856
[14] Salmun, H., Convective Patterns in a Triangular Domain, *Int. J. Heat Mass Transf., 38* (1995), 2, pp. 351-362
[15] Kent, E. F., *et al*., Laminar Natural Convection in Right Triangular Enclosures, Heat *Mass Transf*., *44* (2007), Dec., pp. 187-200
[16] Omri, A., *et al*., Numerical Analysis of Natural Buoyancy-Induced Regimes in Isoceles Triangular Cavities, *Numer. Heat Transf. A*, *52* (2007), 7, pp. 661-678
[17] Roy, S., *et al*., Finite Element Simulation on Natural Convection Flow in a Triangular Enclosure Due to Uniform and Nonuniform Bottom Heating, *ASME J. Heat Transf*er, *130* (2008), 3, pp. 032501
[18] Selimefendigil, F., Oztop, H. F., Numerical Study and POD-Based Prediction of Natural Convection in a Ferrofluids-Filled Triangular Cavity with Generalized Neural Networks, *Numer. Heat Transf. A*, *67* (2015), 10, pp. 1136-1161
[19] Varol, Y., *et al*., Free Convection in Porous Media Filled Right-Angle Triangular Enclosures, *Int. Commun. Heat Mass Transf*., *33* (2006), 10, pp. 1190-1197
[20] Oztop, H. F., *et al*., Investigation of Natural Convection in Triangular Enclosure Filled with Porous Media Saturated with Water Near 4°C, *Energ. Convers. Manage*., *50* (2009), 6, pp. 1473-1480
[21] Varol, Y., *et al*., Influence of Inclination Angle on Buoyancy-Driven Convection in Triangular Enclosure Filled with a Fluid-Saturated Porous Medium, *Heat Mass Transf*., *44* (2008), Mar., pp. 617-624
[22] Basak, T., *et al*., Visualization of Heat Transport during Natural Convection within Porous Triangular Cavities via Heatline Approach, *Numer. Heat Transf. A*, *57* (2010), 6, pp. 431-452
[23] Anandalakshmi, R., *et al*., Heatline Based Thermal Management for Natural Convection Within Right-Angled Porous Triangular Enclosures with Various Thermal Conditions of Walls, *Energy*, *36* (2011), 8, pp. 4879-4896
[24] Saeid, N. H., Natural Convection in Porous Cavity with Sinusoidal Bottom Wall Temperature Variation, *Int. Commun. Heat Mass Transf*., *32* (2005), 3-4, pp. 454-463

[25] Basak, T., *et al*., Natural Convection in a Square Cavity Filled with a Porous Medium: Effects of Various Thermal Boundary Conditions, *Int. J. Heat Mass Transf*., *49* (2006), 7-8, pp. 1430-1441
[26] Mansour, M. A., *et al*., Unsteady Natural Convection, Heat and Mass Transfer in Inclined Triangular Porous Enclosures in the Presence of Heat Source or Sink: Effect of Sinusoidal Variation of Boundary Conditions, *Transp. Porous Media*, *87* (2011), 1, pp. 7-23
[27] Sivasankaran, S., Bhuvaneswari, M., Natural Convection in a Porous Cavity with Sinusoidal Heating on Both Sidewalls, *Numer. Heat Transf. A*, *63* (2013), 1, pp. 14-30
[28] Sivasankaran, S., *et al*., Effect of Moving Wall Direction on Mixed Convection in an Inclined Lid-Driven Square Cavity with Sinusoidal Heating, *Numer. Heat Transf. A*, *69* (2016), 6, pp. 630-642
[29] Nazari, M., *et al.*, Thermal Non-Equilibrium Heat Transfer in a Porous Cavity in the Presence of Bio-Chemical Heat Source, *Thermal Science*, *19* (2015), 2, pp. 579-590
[30] Rahman, M. M., *et al*., Unsteady Mixed Convection in a Porous Media Filled Lid-Driven Cavity Heated by a Semi-Circular Heaters, *Thermal Science*, *19* (2015), 5, pp. 1761-1768

Paper submitted: January 30, 2016
Paper revised: June 16, 2016
Paper accepted: May 21, 2018